Available online at www.sciencedirect.com

ScienceDirect

Advances in Space Research 66 (2020) 219–225

ADVANCES IN SPACE RESEARCH (a COSPAR publication)

www.elsevier.com/locate/asr

GPS loss of lock statistics over Brazil during the 24th solar cycle

Juliana G. Damaceno [a,b,1,*], Karl Bolmgren [c,1], Jon Bruno [c,1], Giorgiana De Franceschi [a], Cathryn Mitchell [c], Massimo Cafaro [b]

[a] Istituto Nazionale di Geofisica e Vulcanologia, Via di Vigna Murata, 605, 00143 Roma, Italy
[b] Department of Engineering for Innovation, University of Salento, Piazza Tancredi, 7, 73100 Lecce, Italy
[c] Department of Electronic and Electrical Engineering, University of Bath, North Rd, BA2 7AY Bath, UK

Received 23 December 2019; received in revised form 6 March 2020; accepted 30 March 2020
Available online 9 April 2020

Abstract

A statistical analysis of Loss of Lock (LoL) over Brazil throughout the 24th solar cycle is performed. Four geodetic GPS dual-frequency (L1, L2) receivers, deployed at different geographic latitudes ranging from about 25° to 2° South in the eastern part of the country, are used to investigate the LoL dependence on time of the day, season, solar and geomagnetic activity. The results of the analysis show that LoL is most likely in the post-sunset hours during summer and equinox, especially within the southern crest of the Equatorial Ionospheric Anomaly (EIA), in a region between about 10°S and 25°S of geographic latitude, matching the typical behaviour of scintillation over Brazil. This is confirmed by the correlation found between the relative occurrence of LoL (LoL (%)) and the Rate Of TEC Index (ROTI), used as a proxy of scintillation index and calculated for each receivers along the entire period of investigation. The LoL (%) for given solar and geomagnetic indices show some correlation with increasing the severity of the index. This correlation is strongest in the area of the southern crest of the EIA, while there is little to no apparent impact closer to the equator, depending on the index. LoL (%) increases with increasing geomagnetic disturbances, varying between ~1% and ~10% for AE ranged between 400 and 1200 nT, and exceeding 3% when Dst is around −100 nT, both related to moderate-severely disturbed conditions.

Keywords: GPS Loss of Lock; Equatorial Ionosphere; Scintillation; 24th solar cycle

1. Introduction

Ionospheric irregularities can cause sudden and rapid fluctuations in the amplitude and phase of electromagnetic waves propagating through them, causing what is known as "ionospheric scintillation". Owing to the morphology of the Earth's magnetic field, scintillations are more likely to occur at high and low latitudes (Kintner et al., 2009). At low latitudes, the "fountain effect" leads to an enhancement of ionization in the regions close to ±15° in magnetic latitude. These enhancements are referred to as the northern and southern crests of the Equatorial Ionization Anomaly (EIA). Ionospheric scintillation is more likely to manifest at the EIA crests as well towards the equator. Brazil is one of the equatorial regions most affected by scintillations, especially at post sunset (see, e.g. Spogli et al., 2013; Cesaroni et al., 2015 and references therein). The scintillation scenario is further exacerbated around solar activity maxima or under severe space weather conditions. For example, during early September 2017 (low solar activity), the EIA southern crest over Brazil intensified and expanded towards higher latitudes as a result of solar flares and coronal mass ejections, leading to a poleward shift of

* Corresponding author at: Istituto Nazionale di Geofisica e Vulcanologia, Via di Vigna Murata, 605, 00143 Roma, Italy.
E-mail addresses: juliana.damaceno@ingv.it (J.G. Damaceno), k.h.a.bolmgren@bath.ac.uk (K. Bolmgren), j.bruno@bath.ac.uk (J. Bruno), giorgiana.defranceschi@ingv.it (G. De Franceschi), c.n.mitchell@bath.ac.uk (C. Mitchell), massimo.cafaro@unisalento.it (M. Cafaro).
[1] These authors have contributed equally to the paper.

https://doi.org/10.1016/j.asr.2020.03.041
0273-1177/

TEC gradients and scintillation (Damaceno et al., 2019 and references therein).

Scintillations lead to a degradation of Global Navigation Satellites System (GNSS) observations and, in the worst case, to Loss of Lock (LoL) of the signal. This causes the receiver to lose track of a transmitting satellite, thus not being able to record any phase or pseudorange observation for the duration of the event. This may affect technological infrastructures relying on space-based navigation systems (see, e.g. Sreeja et al., 2011). By weakening the available satellite geometry, LoL may degrade the precise positioning solution, in terms of accuracy and convergence time. An example of LoL hampering GNSS positioning at low latitude over Africa for selected disturbed days in 2004 is given by Moreno et al. (2011). The authors found LoL to be correlated with large TEC gradients that may lead to scintillations.

Recently, several studies have been carried out to characterise LoL as a function of seasons and for selected geospatial events. In Australia, LoL was investigated by Liu et al. (2017) using scintillation parameters during the solar maximum (from 2011 to 2015). The authors found that LoL is more intense during the equinox months between the evening and midnight, with maxima in 2014. They also investigated the relationship between geomagnetic storms and LoL, concluding that in some cases LoL occurrence increases under severe geomagnetic storms. Over Brazil, Moraes et al. (2018) discussed the relationship between the patterns of scintillation and plasma bubbles, concluding that their alignment along the direction of the magnetic field drives a severe scintillation on the electromagnetic wave crossing them, increasing the possibility of LoL. A similar pattern was found by Dasgupta et al., (2004) in the Indian sector. Rama Rao et al. (2009) investigated the 8–12 November 2014 geomagnetic storms over India. They found that the number of signal phase slips increases with the geomagnetic storms, with severe amplitude scintillation that may cause LoL in the Global Positioning System (GPS) receiver. It is worth noting that phase or cycle slips and LoL were also observed during 6 November 2014, a geomagnetically quiet day selected for comparison, although their occurrence was much lower compared to the disturbed days. Vishnu et al., (2019) also investigated LoL in the Indian sector during the last solar maximum and the results highlighted an increase of LoL during severe geomagnetic storms as well as during the equinox. LoL has also been studied at high latitudes, in northern Scandinavia, by Meggs et al. (2008). The authors explored the differences between LoL due to scintillation and LoL caused by multipath, and indicated that LoL occurrence also depends on the type of receiver.

Inspired by these results and the potentially harmful effects scintillation-induced LoL may have on GNSS, this paper investigates the occurrence of LoL over Brazil for the 24th solar cycle. Phase observations from four GPS receivers, from 2009 to 2018, are used. In Section 2 the data and the method applied are described. Section 3 shows the results in terms of the temporal and spatial distribution of LoL, and its relation to: (1) the Rate Of TEC index (ROTI) (Pi et al, 1997), used as a proxy of scintillation, (2) the solar and geomagnetic activity, as inferred from the solar radio flux at 10.7 cm (F10.7), the Auroral Electrojet index (AE) and the Disturbance storm time index (Dst). Concluding remarks are given in Section 4.

2. Data and method

In this paper, to investigate the correlation of LoL with the solar and geomagnetic activity along the entire 24th solar cycle, the F10.7 (s.f.u.) from 2009 to 2018, the Dst (nT) index from 2009 to 2018, and the AE (nT) index from 2009 to 2017 are considered. Dst is derived from equatorial magnetometer stations and is sensitive to enhancements of the magnetospheric ring current. It is commonly used at low latitudes to identify magnetic storm periods. AE, on the other hand, is mainly considered a high latitude index, and can be a good indicator of the expansion of the auroral ovals towards low latitudes under enhanced geomagnetic activity (see, e.g., Perrone and De Franceschi, 1998). The AE index is used to study the impact of penetrating electric field on the equatorial ionosphere, leading to TEC enhancement (depletion) in the dayside (nightside) ionosphere resulting in an intensification of the EIA in amplitude as well as in latitude (see, e.g. Bagiya et al., 2011 and references therein). F10.7 is used as an indicator of solar activity and mirrors the solar cycle. Hourly values of F10.7, AE and Dst are considered for this study.

It is worth noting that occurrence rate of the different geomagnetic conditions during the 24th solar cycle, the least intense among the recent solar cycles, during which only a few intense geomagnetic storms happened (see, e.g. Watari, 2017; Astafyeva et al., 2018, and references therein). Table 1 reports the occurrence rates of the geomagnetic active periods from 2009 to 2018. Although the range thresholds are chosen arbitrarily, it can still be noted that quiet conditions are mostly prevalent, with only a few cases of extreme or severely disturbed conditions.

Data from four GPS receivers from the International GNSS Service (IGS), located from about 25°S to 2°S in latitude in the eastern part of Brazil, are used to detect LoL in the L1 (1575.42 MHz) and L2 (1227.60 MHz) bands. The geographic location of the four GPS receivers and the percentage of available observations from 2009 to 2018 are depicted in Fig. 1a and 1b respectively. Fig. 1b shows a relatively high and uniform data availability from all four receivers.

LoL events are identified for each receiver and satellite, for L1 and L2 bands together. In a nominal situation, uninterrupted data is expected for visible satellites. A LoL event is considered detected only when no data is logged for visible satellites with elevation above 30°. This elevation threshold is used to minimise multipath effects. However, if all satellites are lost at once for a given epoch, the LoL is discarded and is not analysed, as these losses of signal

Table 1
Occurrence rates of the different geomagnetic conditions (total number of hours and percentage) during the 24th solar cycle determined by Dst and AE hourly indices.

Index	Conditions	Range	Number of cases	Percentage
Dst	Quiet	-20<Dst≤20 nT	69947	79.80%
	Disturbed	-100<Dst≤20 nT	17003	19.40%
	Severe	-250≤Dst<-100 nT	194	0.22%
	Extreme	Dst≤-250 nT	0	-
AE	Quiet	0≤AE<400 nT	70956	89.95%
	Disturbed	400≤AE<600 nT	4886	6.19%
	Severe	600≤AE<1200 nT	2967	3.76%
	Extreme	AE≥1200 nT	79	1.26%

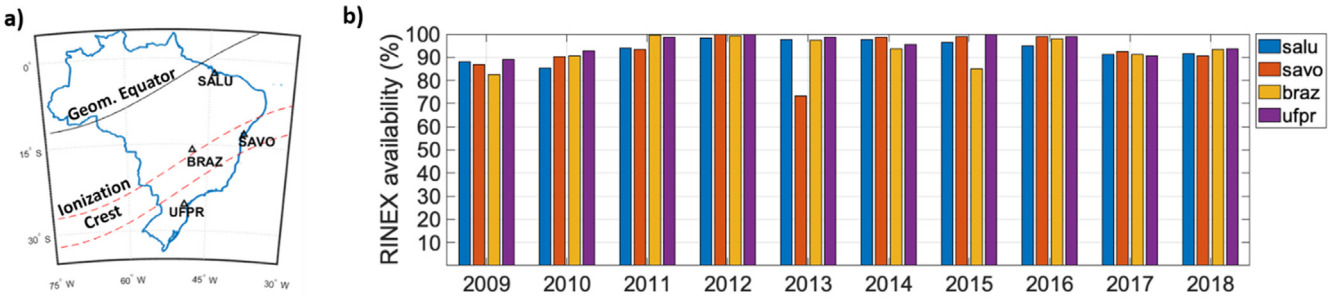

Fig. 1. (a) Geographic location of the four geodetic receivers in Brazil (IGS network) used in the analysis. The magnetic equator (black line) and the region of southern crest of the EIA (dashed red lines) are also plotted; (b) RINEX data availability (%) for each receiver along the period 2009–2018. (For interpretation of the references to colour in this figure legend, the reader is referred to the web version of this article.)

are assumed to be unrelated to the ionospheric activity. In the case of consecutive losses, a single LoL is considered only after a recovery period of uninterrupted data for 5 consecutive minutes. LoL events are grouped by full hour intervals to match the time sampling of the geomagnetic and solar indices.

To determine to which extent the detected LoL are related to ionospheric scintillation, the ROTI (Pi et al., 1997) was calculated for each receiver for the entire period 2009–2018. ROTI is largely used as a proxy for the amplitude scintillation index S4, although some limitations have been highlighted on the correlation between the two quantities. These limitations are mainly due to the fact that ROTI indicates the physical irregularities of ionosphere, while S4 is related to the radio propagation conditions suffering not only the presence of irregularities but also the effective velocity, i.e. a combination between the zonal drift velocity and the velocity of ionospheric pierce point (see, e.g. Liu and Radicella, 2019 and references therein).

To analyse the relation between LoL and ROTI and either of the F10.7, Dst, or AE indices, the relative LoL occurrence (in percentage, LoL (%)) is calculated for predefined bins spanning each index. For ROTI the bins are 0.01 TECu/min wide, for F10.7 each bin is 1 s.f.u. wide, and for AE and Dst the bins are 1 nT wide. For each bin, the number of LoL occurring when the index falls within the bin is divided by the total number of epochs with index values within the bin. For each index bin X_i with edges x_i, denoting by x the measured values of the index, the estimated LoL probability can be written as follows

$$X_i \triangleq [x_i, x_{i+1})$$

$$N_i \triangleq \text{number of epochs with RINEX available when } x \in X_i$$

$$N_{LoL,i} \triangleq \text{number of LoL when } x \in X_i$$

$$P(LoL|x \in X_i) \approx \frac{N_{LoL,i}}{N_i} \quad (1)$$

Because N_i does not take the visibility of the satellite into account, it is scaled by a factor 1/6, which approximates the average time per day one satellite is visible above the 30° elevation mask. This yields the following normalised values used for the analysis,

$$LoL_{X_i}(\%) \triangleq 6 \times P(LoL|x \in X_i) \times 100 \quad (2)$$

3. Results

The main features of the temporal and spatial distribution of the LoL experienced by the four receivers along the 24th solar cycle, are obtained by plotting LoL at the ionospheric pierce point (IPP) at a nominal altitude of 350 km. The results are grouped by season, defined as summer (Nov., Dec., Jan., Feb.), winter (May, Jun., Jul., Aug.) and equinox (Mar., Apr., Sep., Oct.), as well as time of day

in universal time (UT). Fig. 2 shows the number of LoL cases (for L1 and L2 bands together) separately for season, sorted by latitude and time of day (1-degree by 1-hour bins). LoL is more common during summer and equinox (Fig. 2a-b), whilst its signature is weaker in winter. The latitude range where most of the LoL occur is well within the southern crest of the EIA, between about 25°S and 10°S of geographic latitude. We found that LoL in L2 is generally between two and three times more common than in L1, in agreement with Delay et al. (2015) who investigated the loss of lock induced by scintillation on GNSS scintillation monitors. The temporal distribution of LoL shows a marked preference of occurrence at post sunset (21 UT-05 UT, delimited by dashed lines in Fig. 2a-c), which correlates with the typical temporal distribution of scintillations described by several studies over Brazil (see, e.g. Spogli et al., 2013).

To further investigate the correlation between LoL and scintillation along the entire period of analysis, in Fig. 3 the relative LoL occurrence (LoL (%)) for ROTI intervals of 0.01 TECu/min for all detected LoL is plotted. Fig. 3 shows that the probability for LoL, given a certain ROTI, is increasing with increasing ROTI.

To reinforce the possible correlation between LoL and scintillation, Fig. 4 shows the distribution of LoL for each receiver as a function of elevation (a) and azimuth (b). The LoL has a maximum occurrence at elevation angles between 40 and 50° for all receivers but SALU, which has a maximum between 30 and 40°. Despite the existence of an anisotropy of the azimuth direction, the preferred sector is the North one ranging between North-West and North-East (315–360°; 0–45°), for which the receivers located within the EIA southern crest show the highest numbers of LoL. The LoL cluster in the North-West azimuth interval is in agreement with the enhancement of scintillation found over Brazil from an analysis of 32 days of data by Moraes et al. (2018): the scintillation increases predominantly in the direction of the magnetic meridian at azimuth angles around 345° when the signal propagation path segments align with plasma bubbles that are thought to be elongated along magnetic field lines. The reason of

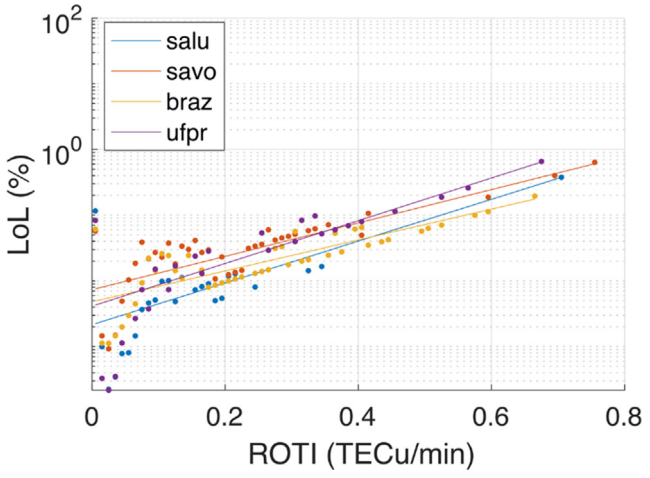

Fig. 3. LoL occurrence probability, LoL (%) (logarithmic scale), vs ROTI throughout the period 2009–2018. LoL (%) is plotted separately for the four GPS receivers together with the proper exponential fitting (continuous lines).

the elevated LoL in the North-East azimuth direction is not clear, and further investigation would be needed to fully explain it. In addition, a possible signature of the impact of the Southern Atlantic Magnetic Anomaly (SAMA) on scintillation and, possibly, on LoL, can be observed in Fig. 4b. In fact, the third maximum in the South-East azimuth direction (135–180°) could be due to the particle precipitation in the SAMA area, which covers most of the South Atlantic. The SAMA would alter the rates of production and recombination of the ionized species, favouring turbulence in the plasma and scintillation (see, e.g., Spogli et al., 2013 and references therein; Abdu et al., 2005).

The LoL (%) as a function of solar and geomagnetic indices is plotted in Figs. 5 and 6, respectively, in semi-logarithmic scale. In order to quantify the relation between $LoL_x(\%)$ and an index x, a least-square exponential fit was applied:

$$LoL_x(\%) = ae^{(b \cdot x)} \tag{3}$$

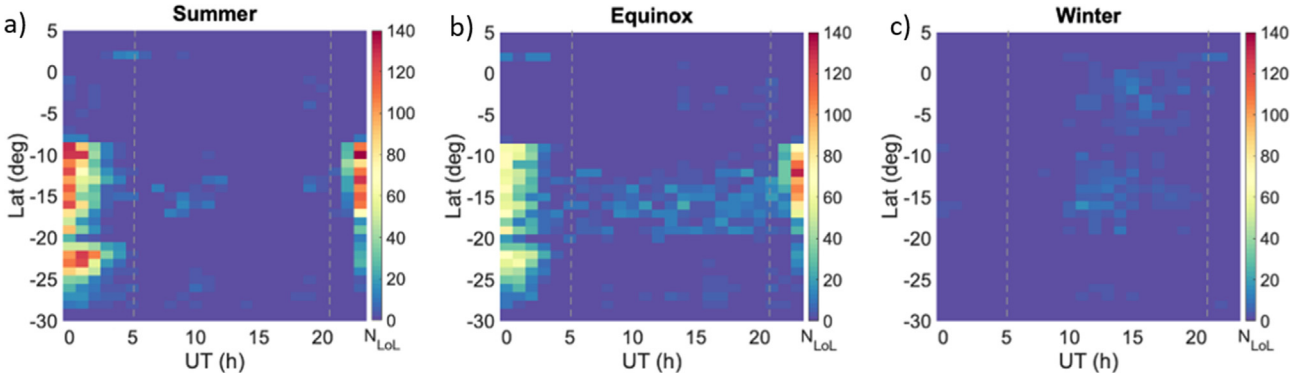

Fig. 2. Latitudinal distribution of the number of LoL cases (for L1 and L2 bands together) vs UT for Summer (a), Equinox (b) and Winter seasons (c) obtained by considering data from 2009 to 2018. The dashed lines highlight the post sunset hours (21UT-05UT), when scintillation is more likely to occur.

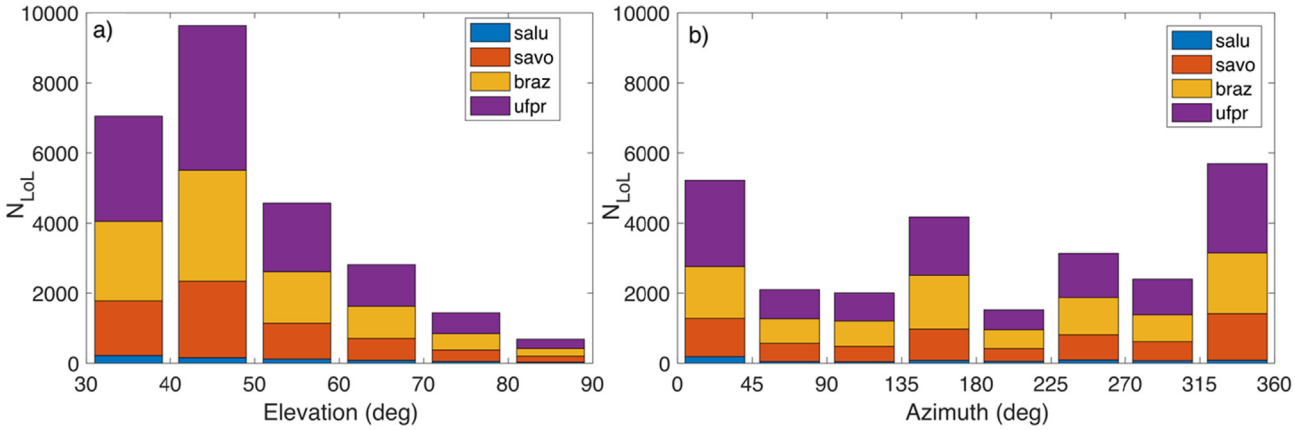

Fig. 4. Total counts of LoL vs (a) Elevation (b) Azimuth. Different colours are associated to different receivers.

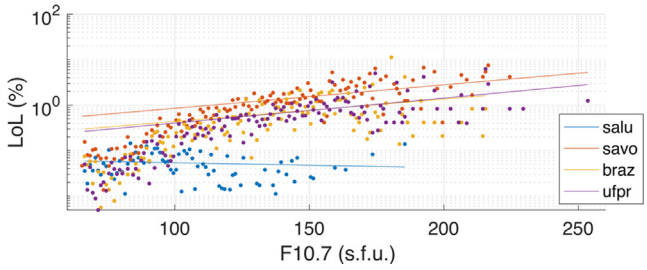

Fig. 5. LoL occurrence probability, LoL (%) (logarithmic scale), vs F10.7 throughout the period 2009–2018. LoL (%) is plotted separately for the four GPS receivers together with the proper exponential fitting (continuous lines).

where a and b are the exponential coefficients evaluated separately for each receiver and index (ROTI, F10.7, AE, Dst). The standard deviation of the residuals between the fit and the data is used as a rough indicator of how well the fit performs. Table 2 summarises the estimated exponential coefficients as well the standard deviation of the residuals for a given receiver and index.

LoL (%) vs F10.7 is plotted in Fig. 5. LoL (%) increases with the solar activity for the receivers within the EIA southern crest, while the LoL at the receiver close to the equator (SALU) appears to be more or less independent of the solar activity.

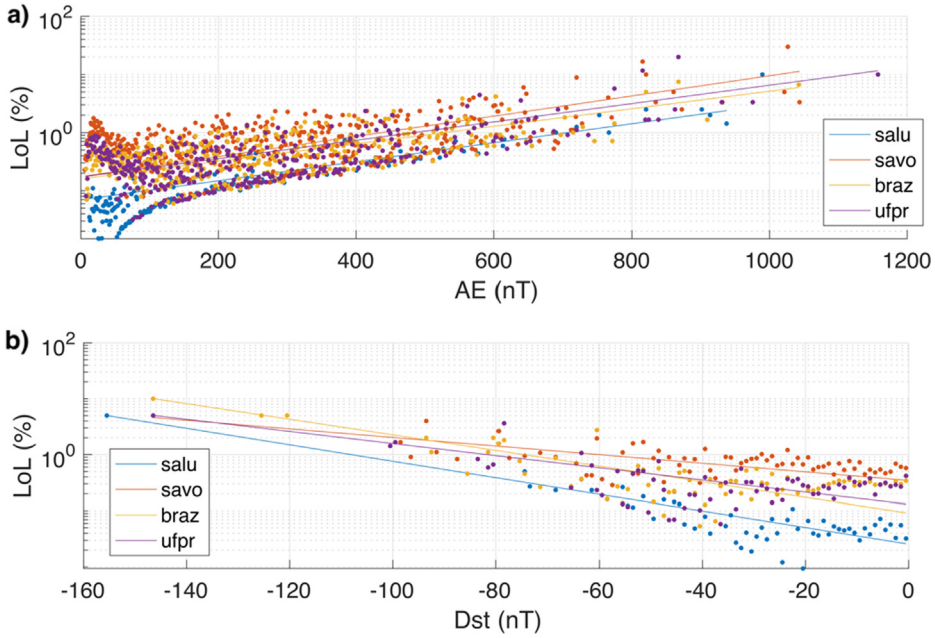

Fig. 6. LoL occurrence probability, LoL (%) (Logarithmic scale), vs geomagnetic indices: a) AE from 2009 to 2017, and b) Dst from 2009 to 2018. LoL (%) is plotted separately for the four receivers together with the proper exponential fitting (continuous lines).

Table 2
Summary of the exponential fits applied to LoL (%) and ROTI, F10.7, Dst, AE indices: fitting coefficients, a and b, together with the Standard Deviation of the residuals (STD) in percent for each fit are given.

	Fit	salu	savo	braz	ufpr
ROTI	a	0.002	0.007	0.005	0.004
	b	7.3	5.8	5.4	7.5
	STD	0.02	0.02	0.01	0.02
F10.7	a	0.07	0.7	0.1	0.1
	b	-0.002	0.01	0.01	0.01
	STD	0.03	1.2	1.1	0.8
Dst	a	0.03	0.3	0.1	0.1
	b	-0.03	-0.02	-0.03	-0.03
	STD	0.04	0.5	0.4	0.4
AE	a	0.07	0.2	0.2	0.2
	b	0.004	0.004	0.003	0.004
	STD	0.1	1.4	0.5	1.1

LoL (%) vs AE and Dst is shown in Fig. 6 (a, b, respectively). A roughly exponential correspondence can be observed between LoL (%) and AE (Fig. 6a), indicating that the probability of LoL increases with AE for all the receivers and reaches up to 10% for severely disturbed conditions (Table 1). LoL (%) also increases as a function of Dst (Fig. 6b): LoL (%) is up to around 3% for disturbed geomagnetic conditions (Dst around −100 nT), as defined in Table 1. It is worth noting that LoL can occur even for quiet geomagnetic conditions.

4. Concluding remarks

In this paper, the relation between Loss of Lock (LoL) and time of the day, season, solar and geomagnetic activity is investigated. Data from four geodetic GPS receivers, deployed at different latitudes in the eastern part of Brazil, is used to retrieve the LoL for the 24th solar cycle, the weakest of the last century. Although the types of receiver hardware and their fields of view vary, the results indicate that the main features of LoL as a function of time of the day and season strongly overlap with the scintillation climatology over Brazil (LoL maxima at post sunset and during summer/equinox). A positive correlation exists between relative LoL occurrence, LoL (%), and ROTI, the proxy amplitude scintillation here used along the entire period analysed. The LoL preferred azimuth direction in the North sector (NW-NE) partially supports a relationship between LoL and scintillation, as it indicates LoL occurrence along the magnetic meridian where the signal propagation path segments align with plasma bubbles. A positive correlation exists between LoL (%), solar activity and geomagnetic disturbances, even if LoL at solar minimum and during quiet geomagnetic conditions is also observed. Close to the equator, LoL (%) does not seem to be correlated with the solar activity. A simple exponential function is found to express empirically LoL (%) as function of ROTI, solar and geomagnetic indices (ROTI, F10.7, AE, Dst). This simple empirical function may be further tested and improved as a function of different latitude and longitude sectors and geomagnetic conditions making use of the available IGS network along different solar cycles, possibly opening up the opportunity of using LoL as a proxy indicator of scintillation.

Acknowledgements

This work was supported by TREASURE project (http://www.treasure-gnss.eu), funded by the European Union's Horizon 2020 Research and Innovation Programme under the Marie Skłodowska-Curie Actions grant agreement No. 722023. CNM acknowledges NERC grant NE/P006450/1. Thanks to the data and index providers: International GPS Service (IGS), the World Data Centre (WDC), Kyoto and CDAWEB (https://www.cdaweb.gsfc.nasa.gov/index.html/). The authors thank the anonymous reviewers who contributed to the general improvement of the paper and Dr. Luca Spogli for the useful discussion on the use of ROTI.

References

Abdu, M.A., Batista, I.S., Carrasco, A.J., Brum, C.G.M., 2005. South Atlantic magnetic anomaly ionization: a review and a new focus on electrodynamic effects in the equatorial ionosphere. J. Atmos. Solar-Terrestrial Phys. 67, 1643–1657. https://doi.org/10.1016/j.jastp.2005.01.014.

Astafyeva, E., Zakharenkova, I., Hozumi, K., Alken, P., Coïsson, P., Hairston, M.R., Coley, W.R., 2018. Study of the equatorial and low-latitude electrodynamic and ionospheric disturbances during the 22–23 June 2015 geomagnetic storm using ground-based and spaceborne techniques. J. Geophys. Res. Sp. Phys. 123, 2424–2440. https://doi.org/10.1002/2017JA024981.

Bagiya, M.S., Iyer, K.N., Joshi, H.P., Thampi, S.V., Tsugawa, T., Ravindran, S., Sridharan, R., Pathan, B.M., 2011. Low-latitude ionospheric-thermospheric response to storm time electrodynamical coupling between high and low latitudes. J. Geophys. Res. Sp. Phys. 116, n/a-n/a. https://doi.org/10.1029/2010JA015845.

Cesaroni, C., Spogli, L., Alfonsi, L., De Franceschi, G., Ciraolo, L., Galera Monico, J.F., Scotto, C., Romano, V., Aquino, M., Bougard, B., 2015. L-band scintillations and calibrated total electron content gradients over Brazil during the last solar maximum. J. Sp. Weather Sp. Clim. 5, A36. https://doi.org/10.1051/swsc/2015038.

Damaceno, J. G., Cesaroni, C., Spogli, L., De Franceschi, G., Cafaro, M., 2019. Multi-instrumental analyses of the September 2017 space weather storm over Brazil. In: 2019 URSI Asia-Pacific Radio Science Conference (AP-RASC). IEEE, New Delhi, India, pp. 1–4. http://dx.doi.org/10.23919/URSIAP-RASC.2019.8738327.

Dasgupta, A., Ray, S., Paul, A., 2004. Errors in position-fixing by GPS in an environment of strong equatorial scintillations in the Indian zone 39, 1–8. http://dx.doi.org/10.1029/2002RS002822

Delay, S.H., Carrano, C.S., Groves, K.M., Doherty, P.H., 2015. A Statistical analysis of GPS L1, L2, and L5 tracking performance

during ionopsheric scintillation, pp. 1–9. https://www2.bc.edu/charles-carrano/delay-ion-pnt2015-labeled.pdf.

Kintner, P.M., Humphreys, T., Hinks, J., 2009. GNSS and Ionospheric Scintillation. Insid. GNSS 4 (4), 22–30 https://www.insidegnss.com/auto/julyaug09-kintner.pdf.

Liu, Y., Fu, L., Wang, J., Zhang, C., 2017. Study of GNSS loss of lock characteristics under ionosphere scintillation with GNSS data at Weipa (Australia) during solar maximum phase. Sensors (Switzerland) 17, 1–15. https://doi.org/10.3390/s17102205.

Liu, Y., Radicella, S., 2019. On the correlation between ROTI and S4. Ann. Geophys. Discuss. 1–14. https://doi.org/10.5194/angeo-2019-147.

Meggs, R.W., Mitchell, C.N., Honary, F., 2008. GPS scintillation over the European Arctic during the November 2004 storms. GPS Solut. 12, 281–287. https://doi.org/10.1007/s10291-008-0090-3.

Moraes, A.de.O., Vani, B.C., Costa, E., Abdu, M.A., de Paula, E.R., Sousasantos, J., Monico, J.F.G., Forte, B., de Siqueira Negreti, P.M., Shimabukuro, M.H., 2018. GPS availability and positioning issues when the signal paths are aligned with ionospheric plasma bubbles. GPS Solut. 22, 95. https://doi.org/10.1007/s10291-018-0760-8.

Moreno, B., Radicella, S., De Lacy, M.C., Herraiz, M., Rodriguez-Caderot, G., 2011. On the effects of the ionospheric disturbances on precise point positioning at equatorial latitudes. GPS Solut. 15, 381–390. https://doi.org/10.1007/s10291-010-0197-1.

Perrone, L., De Franceschi, G., 1998. Solar, ionospheric and geomagnetic indices. Ann. di Geofis. 41 (5–6). https://doi.org/10.4401/ag-3824.

Pi, X., Mannucci, A.J., Lindqwister, U.J., Ho, C.M., 1997. Monitoring of global ionospheric irregularities using the worldwide GPS network. Geophys. Res. Lett. 24 (18), 2283–2286. https://doi.org/10.1029/97GL02273.

Rama Rao, P.V.S., Gopi Krishna, S., Vara Prasad, J., Prasad, S.N.V.S., Prasad, D.S.V.V.D., Niranjan, K., 2009. Geomagnetic storm effects on GPS based navigation. Ann. Geophys. 27, 2101–2110 https://www.ann-geophys.net/27/2101/2009/angeo-27-2101-2009.pdf.

Spogli, L., Alfonsi, L., Romano, V., De Franceschi, G., Francisco, G.M. J., Shimabukuro, M.H., Aquino, M., et al., 2013. Assessing the GNSS scintillation climate over Brazil under increasing solar activity. J. Atmos. Solar-Terrestrial Phys. 105–106, 199–206. https://doi.org/10.1016/j.jastp.2013.10.003.

Sreeja, V., Aquino, M., Elmas, Z.G., 2011. Impact of ionospheric scintillation on GNSS receiver tracking performance over Latin America: introducing the concept of tracking jitter variance maps. Sp. Weather 9. https://doi.org/10.1029/2011SW000707.

Vishnu, T.R., Ratnam, D.V., Priyanka, P.B., Sridhar, M., Raju, K.P., 2019. Detection and Analysis of Cycle Slips from GNSS Observations 29–34. https://www.ijitee.org/wp-content/uploads/papers/v8i4/D2612028419.pdf.

Watari, S., 2017. Geomagnetic storms of cycle 24 and their solar sources. Earth, Planets Sp. 69, 70. https://doi.org/10.1186/s40623-017-0653-z.